AMAS Course on Nondestructive Testing of Materials
NTM'02 – (pp.97–110) – Warsaw, May 20-22, 2002.

Magnetic methods of stress evaluation

B. AUGUSTYNIAK

Faculty of Technical Physics and Applied Mathematics
Gdańsk Technological University
bolek@mifgate.mif.pg.gda.pl

1. Introduction

The aim of this paper is to present a review of non-destructive methods of measurements of residual stress in constructional ferromagnetic materials. The term "residual stress" means the stress influencing considerably more than the range of a single grain. Such stress can be produced in the constructional element either by mechanical load or by thermo-mechanical processing (e.g. welding or grinding). The non-destructive residual stress assessment in steel elements is a matter of great practical importance. When considering the stress detection of ferromagnetic materials it is reasonable to make use of their magnetoelastic properties, especially the influence of the stress on the magnetisation phenomenon. The common characteristic of the magnetic methods is that the investigated material remains under the influence of constant or variable magnetic field and the stress level is evaluated on the basis of a change of certain physical parameter in comparison to its level measured in non-stressed state.

There are many magnetic methods of stress evaluation and they can be divided into three groups considering different methods of stress detection from magnetisation process:

- Straightforward hysteresis loop determination with application of some parameters (maximum of magnetic induction, residual induction and coercive force) or analysis of harmonic components and magnetic anisotropy.
- Application of hysteresis effect itself instead of hysteresis loop investigation with Barkhausen effect and magnetoacoustic emission effect.
- Measurements of non-strictly magnetic quantities like eddy current, ultrasound and leakage field methods.

The paper presents mostly the first two groups of magnetic methods.

2. Modelling of stress – magnetisation dependence

The influence of applied stress on the hysteresis loop have been studied for a long time [1, 5]. However, only in the late 80's was the first uniaxial stress model for ferromagnetic bodies presented [6, 7]. Similar models valid for double-axial stress were proposed at the beginning of the 90's [8]. In the last years the most general double-axis model including every possible angle between stress σ and magnetising force H was proposed [9]. The model introduced by M. Sablik and D. Jiles [8] (model S-J) has been modified several times. This model for uniaxial stress evaluates the magnetisation M – field strength H hysteresis loop dependence $M(H)$ using the inner effective field H_e quantity. The authors of the model assume that there exists an effective field H_e inside the material, depending on σ and M. The influence of residual stress on hysteresis loop is evaluated for known magnetostriction function $\lambda(M)$. Considering that σ and M are parallel, Sablik and Jiles calculate the effective field as:

$$H_e = H + \alpha M + \frac{3}{2}\frac{\sigma}{\mu_0}\frac{\partial \lambda}{\partial M} \tag{2.1}$$

where the second term (αM) describes the impact of magnetisation and the third component describes the change of magnetoelastic energy W_m.

A hysteresis loop $M(H)$ is partially described by anhysteretic component $M_a(H)$, which corresponds to the process of magnetisation without energy dissipation. However, the dissipation is always present, so M is always different from M_a:

$$M = M_a - \delta k \frac{dM}{dB_e} \tag{2.2}$$

where the coefficient k is the parameter proportional to the density of defects "pinning" the magnetic domain walls (DW). Next, $B_e = \mu_0 H_e$ and δ is a parameter equal to $+1$ or -1 depending on magnetic field direction. Anhysteresis magnetisation $M_a(H_e)$ is assumed to be like sigmoidal and the authors of the model S-J apply the Langevin's function $L(x)$:

$$M_a = M_s\, L(H_e/a) \tag{2.3}$$

where: M_s is a saturation magnetisation, $L(x) = \coth(x) - 1/x$, the parameter a is comparable with the value of coercive force H_c. It was assumed that magnetisation M is a sum of a non-reversible movements component M_n and reversible movements component M_o. It was also assumed that reversible component M_o is proportional to the difference $\Delta M = M_a - M_n$ with the coefficient of proportionality c, $(c < 1)$. The non-reversible component dM_n change caused by the field strength increase dH is described by

the following equation:

$$\frac{dM_n}{dH} = \frac{\Delta M}{\frac{\delta k}{\mu_0} - \left(\alpha - 1.5\frac{\sigma}{\mu_0}\frac{\partial^2\lambda}{\partial^2 M^2}\right)\Delta M}. \tag{2.4}$$

For the alternating field strength the numerical solution of Eq. (2.4) represents hysteresis loop of non-reversible movements component M_n from which hysteresis loop of magnetisation M is deduced. The S-J model describes thus the hysteresis process applying five parameters, whose values depend on material type. These parameters are the following : 1 – M_s, 2 – α, 3 – a, 4 – k and 5 – c. To determine the stress dependence of magnetisation process, the $\lambda(M)$ function as second-order polynomial is used.

An example of a hysteresis loop $M(H)$, evaluated by the author [10] for the three levels of residual stress σ are shown in Fig. 1. The following parameter values were taken for the calculations: $M_s = 1.35 \cdot 10^6$ A/m, $\alpha = 20 \cdot 10^{-4}$, $a = 2000$ A/m, $k\,\mu_0 = 2000$, $c = 0.5$.

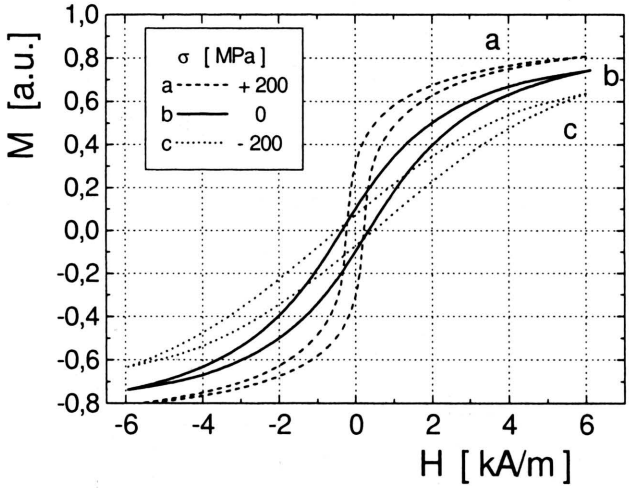

FIGURE 1. Hysteresis loops, calculated by the author for the three levels of residual stress.

For $\lambda(M)$ dependence, a second-order polynomial form was taken with typical for steel $\lambda_s = 8 \cdot 10^{-6}$ value of λ parameter for $M = M_s$.

These calculated changes of hysteresis loops due to stress agree qualitatively with experimental results [2]. This can be illustrated by the examples of hysteresis loops shown in Fig. 2. The results were obtained for the low-carbon XC10 steel containing about 0.06-0.14 (wt) % of carbon. Magnetic

field strength H was altered with constant period $T = 10\,\mathrm{s}$ and magnetic field and stress were parallel [11]. Mechanical load was applied using push-pull machine made at INSA by Chicois [12]. The plots in Figs. 1 and 2 reveal that the tensile stress causes the increase of the magnetisation rate and also results in narrowing of the hysteresis loop. The opposite effect is observed while the compressive stress is applied. Using the S-J model it was possible to calculate stress induced changes of some main parameters of hysteresis loop. Such results are shown in Fig. 4.

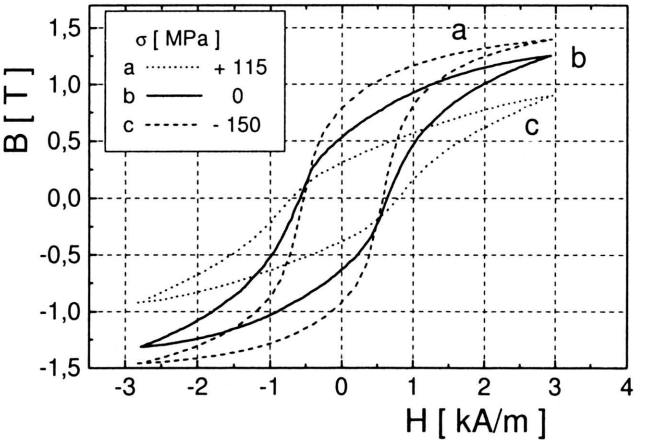

FIGURE 2. Magnetic hysteresis loop versus stress measured in low-carbon XC10 steel.

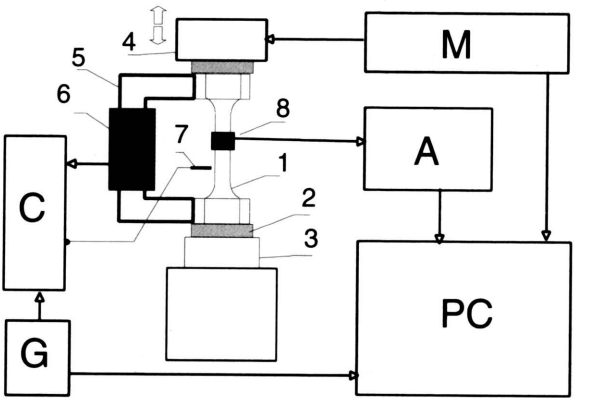

FIGURE 3. The block diagram of the set-up applied to fundamental investigation of magneto–elastic properties of steel.

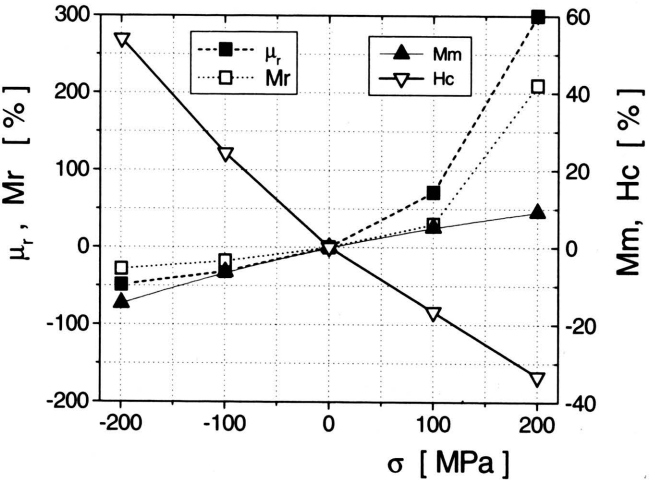

FIGURE 4. The relative changes of parameters of hysteresis loop caused by the stress applied to the sample, calculated by Eq. (2.4).

Figure 4 presents relative changes of four basic parameters, i.e. : μ_r – maximum of magnetic permeability, M_r – residual magnetisation, M_m – maximum of magnetisation, H_c – coercive force. The presented parameter values are related to the unstressed state. The plots drawn in Fig. 4. show the fact that stress increase leads to monotonous increase of first three parameters and to decrease of the fourth parameter (coercive force). Relative changes of μ and M_r are significantly greater than changes of coercive force and maximum of magnetisation.

The investigation of hysteresis loop in the case of bi-axial stress was made by Langman [13] who he proved that stress σ_2 applied perpendicularly to σ_1 decreases the magnetisation strength along σ_1. Decrease of magnetic permeability and maximum of magnetisation was also observed. Tensile stress σ_2 perpendicular to the magnetisation direction results at the same time in a lower value of residual induction B_r. These effects were explained qualitatively by bi-axial stress model of Sablik [8]. The latter model is a modified version of S-J model, described above, and includes references to microscopic Schneider model [14] which had been proposed earlier. Schneider assumed uni-axial stress state and magnetisation was calculated taking random domain distribution in stressed and magnetised body.

Hysteresis loops of ferromagnetic body can be also described by recently proposed Hauser statistical model [15, 16]. This model includes both random domain volume and magnetisation vector directions distribution and also enables for the investigation of uni-axial stress influence on magnetisation

process. In another paper [17] of Sablik at al. a case of non – coaxial stress – magnetic field directions was modelled and investigated. This research had proved that for isotropic material there is a certain angle between stress and magnetisation vector and that applied stress has no influence on the shape of hysteresis curve.

3. Measuring of hysteresis loop properties

While testing magnetic properties of a material, and especially when hysteresis loop $B(H)$ is in question, the uniform magnetisation is required. Such a condition can be fulfilled in laboratory arrangements using a proper sample configuration and a special magnetising set-up. Such required equipment where magnet yoke was applied is shown in Fig. 3. In field applications it is possible to apply only a C-shaped electromagnet to magnetise a part of a construction. The voltage induced in the pick-up coil placed on the core of the electromagnet is integrated in order to evaluate the magnetisation level. Unfortunately, this voltage signal reflects the flux density rate in the core rather than the real flux passing through the magnetised material. The magnetic induction level in the material depends strongly on its geometry and it is modified by the eddy current effects that are generated by the flux alternations. This is the reason of a very poor correlation between the induced voltage and magnetic properties of investigated material, even at low rates of magnetisation speed. Having applied a proper calibration procedure, it is however possible to register the relative changes of hysteresis loop parameters and determine the residual stress level. The portable equipment to investigate hysteresis loop parameters was designed by D. Jiles at laboratory of AMES [19]. No practical applications of this apparatus have been reported so far. It should be observed that usage of a yoke electromagnet is problematic when applied to curved surfaces. A gap between a yoke pole and the curved surface causes a flux density loss. To minimise this problem a magnetic jelly coupler was applied at AMES. The same problem has been fully solved at Gdańsk Technical University using a yoke electromagnet consisting of movable plates adopting themselves to the shape of investigated element [20].

The second group of magnetic methods dealing with indirect detection of hysteresis loop properties contains two methods:

1. where harmonic components of the induced voltage are analysed,
2. where magnetic anisotropy is detected.

The method of harmonic components was designed by Kwun and Burkhard of SWRI (San Antonio) [21, 22]. The voltage signal is induced in a coil placed

in proximity of a magnetised specimen. The material is magnetised using an excitation coil as it is shown in Fig. 5.

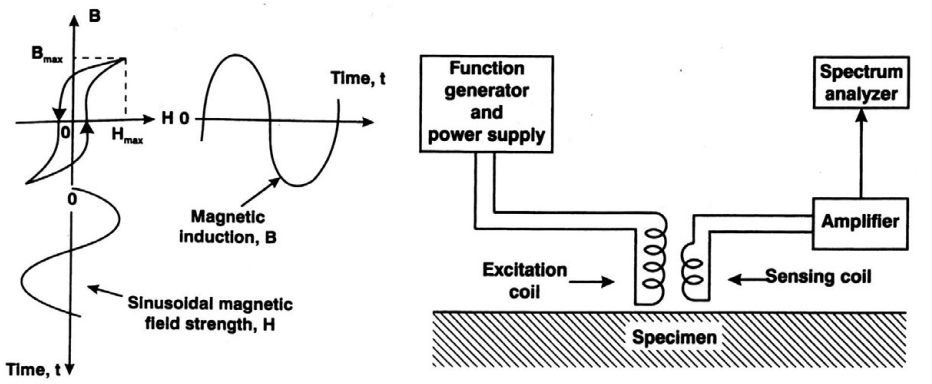

FIGURE 5. Method of harmonic components measurement.

The idea of the method is presented on the left side of Fig. 5 and the block – diagram of the instrumentation on its right side. Because of nonlinear character of hysteresis loop the voltage excited in sensing coil includes a variety of harmonic components. This voltage signal is processed in a spectrum analyser.

To determine magnetisation level in the specimen the value of third harmonic of analysed signal is calculated. The frequency of the magnetising signal lies in the range of 10 Hz. The relative change of the output signal caused by the applied stress within the elastic region is on the order of $\pm 40\%$, when compared to the unstressed state. The method can be applied up to 50% of the yield limit. Kwun and Burkhard used the described method to examine different objects (i.e. pipelines, rails) and claimed that the method is useful for rapid and automated inspection of residual stresses. It is possible to penetrate the structure within depth of some millimetres using different frequency of the magnetising signal.

Detection of magnetic anisotropy is the method at which stress induced angular distribution of the magnetisation of the specimen is deduced. Two methods of such an anisotropy detection have been designed. They are presented in Fig. 6. At the left side there is the one devised by Kishimoto's [23], using a ferrite cored coils placed perpendicularly to the specimen's face. At the right side there is Langman's [24] system with two sets of air coils placed in parallel to the specimen face. Kishimoto detects the magnetisation anisotropy using a set of two coils connected in series while their winding direction is opposite. The specimen is magnetised by a yoke core. The de-

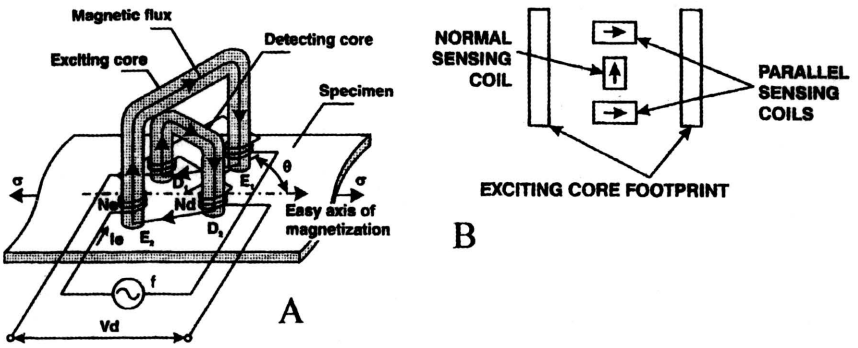

FIGURE 6. Two arrangements for measuring magnetisation anisotropy.

tecting core with sensor coils is placed symmetrically to the axis joining the yoke core poles. Langman uses magnetising field frequency on he order of 100 kHz and the measured signal is analysed using a bulit-in amplifier. Increase of stress up to the "elastic" limit leads to relative change of the output signal of about 10% [25, 26]. To avoid the influence of the crystallographic anisotropy on output signal a differential method of detection is used: data are taken for two perpendicular directions of coils geometry. Magnetisation anisotropy method was applied to detect residual stresses in rails and for welds inspection [25].

4. Methods related to hysteresis effect

There are two physical effects related to the magnetisation "jumps" caused by an abrupt movement of the magnetic domain wall (DW). These effects are:

1. rapid change of magnetic induction at the specimen surface,
2. the acoustic (stress wave) pulse travelling to the surface.

The first effect it is the classical effect named 'Barkhausen effect' (est. 1919) [18, 27]. More correctly this should be named as a 'field Barkhausen effect' to distinguish it from the 'mechanical Barkhausen effect', caused by the dynamical stress applied to a specimen under investigation [28, 29]. Voltage signals for these both effects are induced at pick-up coils placed in proximity of the tested material surface. The 'acoustic' effect is named as a 'magnetoacoustic emission' and voltage signal is provided by a piezoelectric sensor placed on the specimen surface [30].

A Barkhausen effect (BE) is caused by the step-wise movements of magnetic DW mainly between domains with polarisation vectors pointing the opposite directions. The changes of BE intensity can be caused by the changes of this DW population at stressed material. The BE intensity should increase for tensile load and decrease when the material is compressed. An example of BE intensities for low carbon steel (XC10) is shown in Fig. 7. It is the case of uni-axial stress parallel to magnetisation direction. The experimental conditions were similar to that shown in Fig. 3.

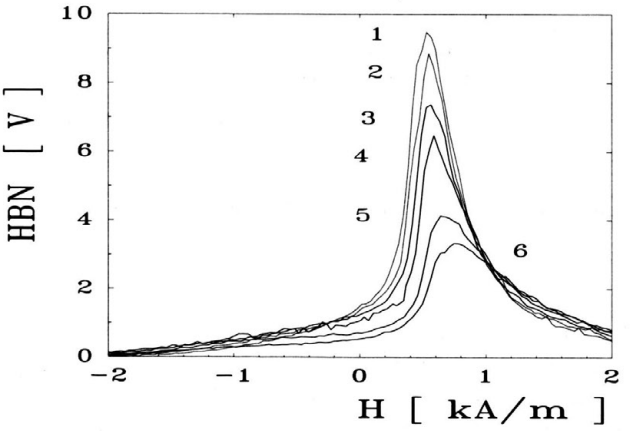

FIGURE 7. Results of measurements of Barkhausen effect in steel under following stress levels: (1) +115 MPa, (2) +50 MPa, (3) 0 MPa, (4) -37 MPa, (5) -104 MPa, (6) -167 MPa. Stress was uni-axial and parallel to magnetisation direction.

A pick-up coil wound on the specimen provides voltage signal from which the BE voltage signal is extracted. The BE intensity was evaluated by means of integrating BE voltage component. This intensity was marked on the vertical axis as HBN. Figure 7 presents a part of hysteresis loop containing BE signal registered during increase of field strength. As presented results show distinct changes of BE level as a function of field strength H occur. Maximum of this function increases as a function of tensile stresses and decreases as a function of compressive stresses and therefore the BE intensity maximum (parameter PM) can be treated as a parameter suitable to describe stress dependence of BE intensity.

This dependence obtained for the steel XC10 is presented in Fig. 8. One can find that the PM level saturates at stress level on he order of ±200 MPa, which is close to the yield stress parameter of tested steel.

High dynamics of stress dependence of BE intensity is essential for precise stress evaluation. Figure 8 reveals that the PM parameter for the XC10

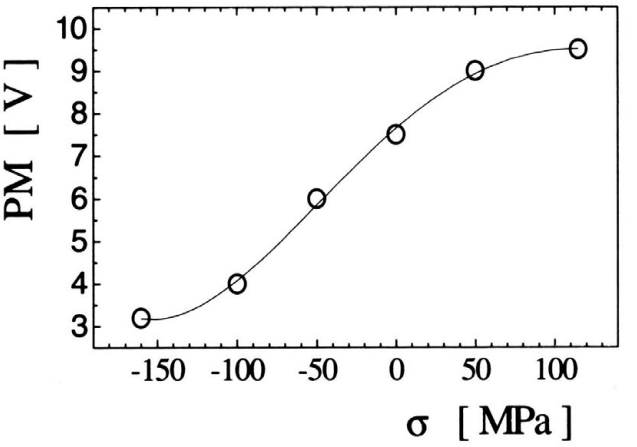

FIGURE 8. The uni-axial stress dependence of BE intensity given by PM parameter for XC10 steel.

steel ratio of tensile and compression state is on he order of 3. A significant improvement of stress sensitivity can be achieved using the BE pulse counting method. Such a method was developed at Gdańsk Technical University [31].

In the field conditions the EB signal measurement is done using the local magnetisation by the C shaped electromagnet. The BE voltage signal is detected by pick-up coil placed in proximity of the magnetised surface.

The block-diagram of the instrumentation developed in Faculty of Physics of Gdańsk Technical University for such BE measurements is shown in Fig. 9. An electromagnet core (2) with driving coil (3) touches the investigated surface (1). A voltage signal of BE effect is induced in sensor coil wound around the ferrite core (4). An auxiliary coil (5) is used to control the electromagnet magnetisation level. The entire probe /(2) to (5)/ is connected to the measuring unit which is coupled via interface (IF) to the personal computer (PC). The measuring unit consists of the generator (G) of the magnetising current, current power amplifier (A), BE signal preamplifier (B) and BE signal analyser (UA). The latter includes band-pass filters, AC/DC converters, and pulse amplitude analysers. The amplifier (C) in Fig. 9 is used to process a signal generated in auxiliary coil. This measuring set enables storage of two signals:

1. the BE intensity,
2. the BE pulse count rate hysteresis.

The pulse counts sum per magnetisation cycle, denoted as N_C parameter, depends on the adjusted threshold level. The important factor of a proper

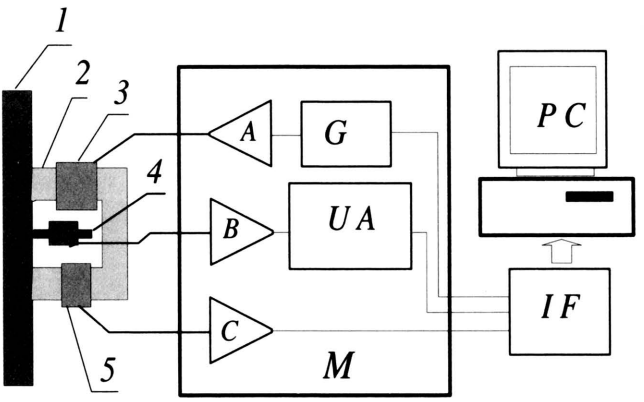

FIGURE 9. Block-diagram of the instrumentation used to Barkhausen effect measurements.

measuring procedure is to adjust a threshold level in order to achieve two goals: the maximum of dynamics N_C versus applied stress and minimum of the standard deviation of N_C for its lowest values. This procedure is applied in order to measure the bi-axial stress dependence calibration function $N_C(\varepsilon_x, \varepsilon_y)$ for each tested steel. An example of such a function obtained for St3 grade steel is shown in Fig. 10.

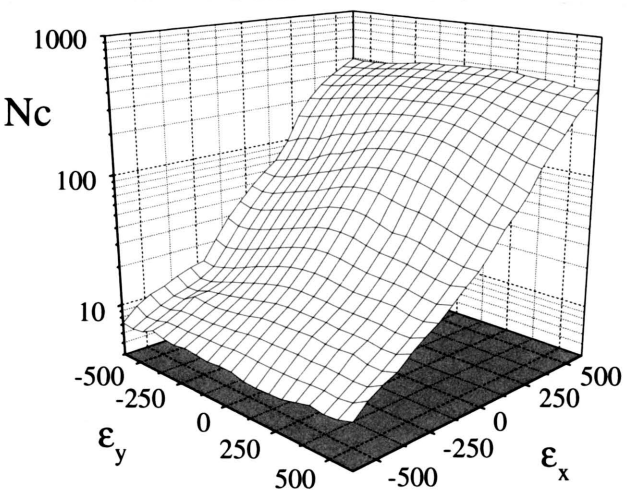

FIGURE 10. A calibration function $N_C(\varepsilon_x, \varepsilon_y)$ of the Barkhausen signal measured for different strain levels.

Examples of the application of the described equipment to residual stress distribution are shown in Figs. 11 and 12. These results deal with residual stress occurring in welded plates. Two plates were joined with butt weld. The BE intensity (given by N_C parameter) was measured at each point at two directions:

1. along the line parallel to the weld seam (x-axis),
2. along the direction perpendicular to the weld seam (y-axis).

The stress level at each point was calculated using the calibration function $N_C(\varepsilon_x, \varepsilon_y)$ and these two values of N_C. Figure 11 presents distribution of N_C at x-direction of the field and Fig. 12 presents the calculated distribu-

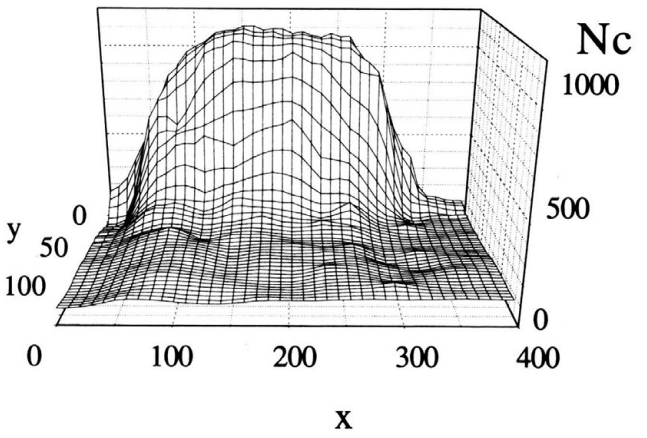

FIGURE 11. Distribution of N_C parameter measured over the welded plate. Magnetic field H is parallel to the x-axis (x and y are in mm).

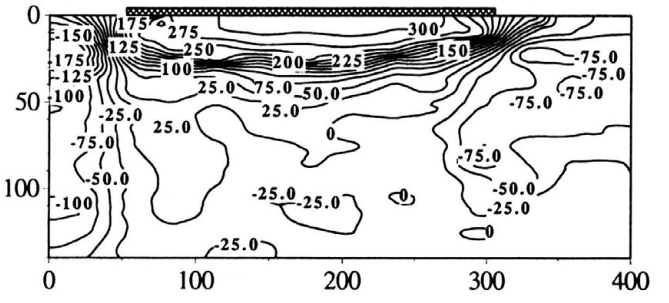

FIGURE 12. The iso-lines of σ_x [MPa] stress component distribution over the welded plate.

tion of stress component parallel to the weld seam. These distributions are well consistent with predictions and also quantitatively correlated with stress distribution calculated for these plates with FEM procedure [33].

5. Conclusions

This review shows that many magnetic methods of stress detection are proposed but the most advanced and promoting is the BE-based method. This method has been now enhanced by bi-axial model of BE stress dependence [9]. Practical application of this method is however reduced to near surface layer stress detection. Bulk stress distribution evaluation will be probably possible using the MAE [20].

References

1. R.M. BOZORTH, *Ferromagnetism*, 1961.
2. D. JILES, *Introduction to Magnetism and Magnetic Materials*, Chapman and Hall, 1991.
3. E.W. LEE, *Reports on progress in physics*, Vol.18, No.184, 1955.
4. B. AUGUSTYNIAK, *Materiały - I Krajowa Konferencja "Podstawy Fizyczne Badań Nieniszczących", Gliwice 1995*, pp.5-23, 1995 (conference paper in Polish).
5. A. HERPIN, *Theorie du Magnetisme*, 1968.
6. M.J. SABLIK, H. KWUN, G.L. BURKHARDT and D.C. JILES, *J. of Appl. Phys.*, Vol.61, No.8, Pt.2B, 3799-3801, 1987.
7. M.J. SABLIK and D.C. JILES, *IEEE Trans. on Magn.*, Vol.29, No.4, pp.2113-2123, 1993.
8. M.J. SABLIK, L.A. RILEY, G.L. BURKHARDT, H. KWUN, P.V. CANNELL, K.T. WATTS, R.A. LANGMAN, *J. of Magn. Magn. Mater.*; Vol.132, No.I-3, pp.131-148, 1994.
9. M.J. SABLIK, B. AUGUSTYNIAK, M. CHMIELEWSKI, *J. of Appl.Phys.*, Vol.85, No.8, pp.4391-4393, 1999.
10. B. AUGUSTYNIAK, *Materiały - II Krajowa Konferencja "Podstawy Fizyczne Badań Nieniszczących"*, pp.7-12, 1997 (conference paper in Polish).
11. M.J. SABLIK and B. AUGUSTYNIAK, *J. of Appl.Phys.*, Vol.79, No.2, pp.963-972, 1996.
12. J. CHICOIS, *Thesis*, INSA de Lyon, France 1987.
13. R. LANGMAN, *IEEE Trans. Magn.*, Vol.26, No.4, pp.1246-1251, 1990.
14. C.S. SCHNEIDER, P.V. CANELL, K.T. WATTS, *IEEE Trans. Magn.*, Vol.28, No.5, pp.2626-2631, 1992.
15. H. HAUSER, *J. of Appl.Phys.*, Vol.75, pp.2584-2597, 1994.
16. H. HAUSER, R. GROSINGER, *J. of Appl.Phys.*, Vol.85, No.8, pp.5133-5136, 1999.

17. M.J. SABLIK, S.W. RUBIN, L.A. RILEY, D.C. JILES, D.A. KAMINSKI, S.B. BINER, *J. of Appl. Phys.*, Vol.74, No.1, pp.480-488, 1993.

18. J. DEPUTAT, *Nieniszczące metody badania materiałów*, Gamma 1997.

19. A. PARAKKA and D.C. JILES, *J. Magn. Magn. Mat.*, 140-144, Pt.3, 1841-1842, 1995.

20. B. AUGUSTYNIAK, M. CHMIELEWSKI, M.J. SABLIK, *Nondestructive Testing and Evaluation*, Vol.17, No.6, pp.351-361, 2001.

21. H. KWUN, G.L. BURKHARDT, E.G. SMITH, *Rev.Progr. Quant.NDE*, D.Q. Thompson and D.E.Chimenti (Eds.), Vol.9, pp.1895-1903, 1990.

22. H. KWUN, G.L. BURKHARDT, *NDT International*, Vol.20, pp.167-171, 1987.

23. S. KISHIMOTO, M. HANABUSA, W. WAKIWAKA, H. YAMADA, *IEEE Trans.J.Magn*, Vol.7, pp.269-273, 1992.

24. M.J. Sablik, B. Augustyniak, *Wiley Encyclopedia of Electrical and E1ectronics Engineering. Magnetic Methods of Nondestructive Evaluation*, Webster, Ma-Mi, pp.12-30, 1999.

25. *Hanbook of measurement of residual stresses*, J. Lu (Ed.), The Fairmont Press Inc., 1996.

26. R. LANGMAN, *NDT Intl.*, Vol.16, pp.59-65, 1983.

27. T. PIECH, *Badania Magnetyczne – Wykorzystanie Efektu Barkhausena*, Gamma 1998.

28. B. AUGUSTYNIAK, *Emisja Magnetomechaniczna. Emisja Akustyczna*, 417; ed.IPPT, 1994.

29. B. AUGUSTYNIAK, M. CHMIELEWSKI, J. CHICOIS, *Editions de Physique. J. de Physique IV*, Vol.6, No.8, pp.541-544, 1996.

30. B. AUGUSTYNIAK, *J. Magn.Magn. Mater.*, 196-197, 799-801, 1999.

31. B. AUGUSTYNIAK, *Badania Nieniszczące*; Vol.5, pp.17-23, 1996.

32. B. AUGUSTYNIAK, M. CHMIELEWSKI, W. KIELCZYŃSKI, M.J. SABLIK, *Proc.IX Conf. AMME*, Sopot 2000.

33. W. KIEŁCZYŃSKI, B. AUGUSTYNIAK, M. CHMIELEWSKI, *Proc. 3rd Int. Conf. on Barkhausen Noise and Micromagnetic Effects*, A. Wojtas (Ed.), Tampere 2001.